Proc. of WESIC 2001, University of Twente, The Netherlands, 27-29 June 2001

SEAM TRACKING FOR LASER WELDING WITH AN INDUSTRIAL ROBOT

G.R.B.E. Römer

University of Twente, Chair of Applied Laser Technology
Dept. of Mechanical Engineering, P.O. Box 217, 7500 AE Enschede
The Netherlands
email: g.r.b.e.romer@wb.utwente.nl

Abstract

Because of their construction and flexibility, industrial robots are suitable to be used, with a laser source and an optical fiber, for laser welding of 3D products. However, the positioning accuracy of robots are insufficient for laser welding. Also the product and clamping tolerances are too wide for laser welding. These problems can be solved by applying sensors, which measure the location of the seam in real-time.
This paper describes the integration and performance of a commercial seam tracking sensor with an industrial 6DOF robot.

1 Introduction

High power laser welding of metal parts has several advantages over conventional welding techniques. The good focussing characteristics of a laser beam and the associated high power density in the focus, result in high welding velocities (up to 250mm/s). Other advantages are a large depth-width ratio of the weld, and a weld which meets high optical demands. Continuous laser welding is more and more applied for joining of sheet metal plates. Due to the advantages of laser welding, there is an increasing industrial interest to apply laser welding also for joining of 3D products. For this purpose, a Nd:YAG laser source with an optical fiber and a robot is very convenient, see figure 1. However, industrial robots can not be applied directly, because of their limited positioning accuracy (OldeBenneker 2000a). Prior research showed that for laser welding of steel, using a 300 μm diameter laser spot, positioning tolerances are smaller than 100μm (OldeBenneker 2000b). The small beam diameter also imposes exacting demands on the on part tolerances and clamping tools. In addition, the seam geometry may change during welding due to thermal distortions. These positioning errors can be compensated for by linking a seam detection sensor to the course of the seam, see figure 1. Such a seam tracking system can correct the position of the laser focus in relation to the seam, thus achieving a precise positioning capability.

Seam tracking is more and more applied for welding straight seams in sheet metal plates. Commercial seam tracking sensors, are optimized for this relatively simple configuration. This paper describes the adaptation, integration and performance of

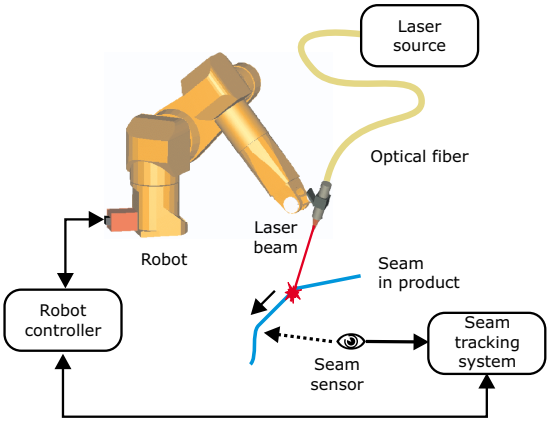

Figure 1: Configuration of a laser welding production cell, composed of a laser source a robot, and a seam tracking system.

such a commercial system with a 6DOF robot for welding of non-straight seams in 3D products, which comprises:

- a method, to calibrate the Tool Center Point (TCP), of the sensor and the laser beam (focus),
- a method to track a seam in 6 coordinates.

2 Experimental setup

The robot used is a STÄUBLI RX90 robot with 6 DOF, see figure 2(a). Its absolute positioning accuracy is $\Delta_r = \pm 50\mu$m, its repeatability $\pm 20\mu$m. To the wrist of this robot, a FALLDORF seam detection sensor is attached. This optical sensor, applies active triangulation to measure the seam location, see figure 2(b). Using a laser diode and a cylindrical lens, a line is projected on the seam. Its reflection is captured by an imager (camera). Because, the optical axes of projection and observation are under an angle $\alpha \approx 50^\circ$, height and shape of the product (seam) can be derived from the camera image. In total 49 geometrical characteristics of the seam are extracted by image processing, at a rate of 200Hz. These quantities are defined relative to the coordinate system of the sensor, see figure 2(b). Three coordinates of the seam, at the point where the diode laser beam intersects to the seam, can be used for TCP calibration and seam tracking: the y_s, and z_s-location (both at an accuracy of $\Delta_s = \pm 40\mu$m), as well as the angle ρ_s (accuracy $\pm 3^\circ$) between the y_s-axis and the product surface (rotation about the x_s-axis). Note that the x_s-axis was chosen to be tangent with the seam. From the z_s-location, the x_s-location of the seam is calculated, $x_s = z_s/tan(\alpha)$, by the robot-controller, to which the sensor is attached.

3 Tool Center Point calibration

The need for Tool Center Point calibration For accurate determination of the location of the seam in robot (or world) coordinates, the exact position and orientation of the Tool Center Point (TCP) of the seam detection sensor, relative to the robot face

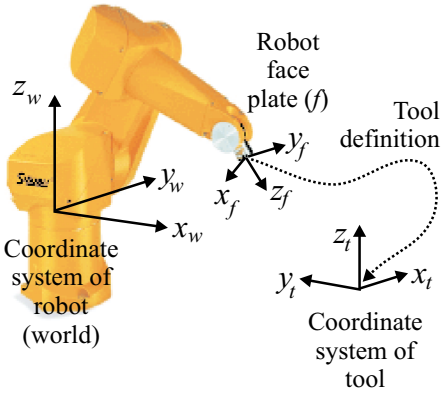

(a) STÄUBLI RX90 robot and its coordinate systems.

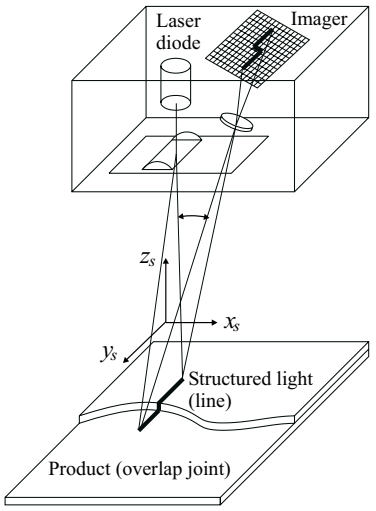

(b) Principle of the FALLDORF seam detection sensor and its coordinate system (subscript s).

Figure 2: The robot and the seam detection sensor.

plate, must be known. The (six-dimensional) transformation describing this position and orientation is usually referred to as the *tool* definition, see figure 2(a). Similar, for accurate positioning of the focus of the high-power Nd:YAG laser beam on the seam, the exact position and orientation of the focus relative to the robot face-plate must be known.

Postition and orientation of the tool The laser welding process is quite tolerant with respect to orientation errors of the laser beam. Therefore, the orientation of the tool (sensor as well as laser beam) can be derived from the dimensions of the laser focusing optics and of the sensor. This is usually sufficiently accurate, such that the orientation of the tool needs not to be calibrated. However, the location of the origin of the tool, relative to the robot face-plate (i.e. x, y, z), needs to be known at an accuracy better than 100μm. In the following, a method to calibrate these components of the tool definition is discussed. It is is based on a patent for TCP calibration of spot welding guns (Thorne 1999). First, the method is described for the TCP calibration of the sensor.

Tool definition The tool definition (or TCP) is defined (here) by

$$TOOL = trans(x, y, z, \varphi, \phi, \rho) \tag{1}$$

It is composed of a translation over (x, y, z) along the corresponding axis of the coordinate system of the robot face-plate, to fix the origin of the tool, and three rotations to fix the orientation of the tool. The rotations are defined (here) by a rotation *yaw* (i.e. a rotation of φ degrees about the z_f-axis of the face plate), a rotation *pitch* (i.e. a

rotation of ϕ degrees about the y-axis of the tool, after yaw rotation has been applied), and finally a rotation roll (i.e. rotation of ρ degrees about the z-axis of the tool, after yaw as well as pitch have been applied). As mentioned, it is assumed that φ, ϕ and ρ are known. The initial (or assumed) translation components (x, y, z) may be obtain from the dimensions of the sensor and its mount to the wrist of the robot.

TCP calibration The real (R) tool definition may differ from the assumed (A) tool definition, i.e. the origin of the two are spaced by a vector $\mathbf{V} = [V_x, V_y, V_z]$, see figure 3(a). If $V_x = V_y = V_z = 0$, the TCP is calibrated. If not, the TCP must be calibrated.

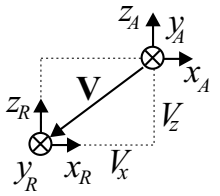

(a) The real TCP (R) is spaced by a vector $\mathbf{V}$ from the assumed TCP (A).

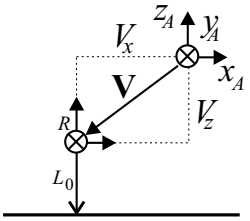

(b) L_0 is the distance of the real TCP to the calibration plate S.

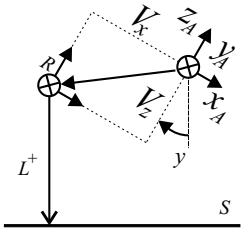

(c) L^+ is the distance of the real TCP to the calibration plate S, when the robot is rotated $+\theta_y$ about the y_A-axis of the assumed TCP.

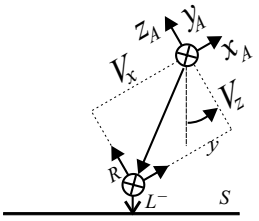

(d) L^- is the distance of the real TCP to the calibration plate S, when the robot is rotated $-\theta_y$ about the y_A-axis of the assumed TCP.

Figure 3: The vector $\mathbf{V}$ and 3 orientations of the TCP's to determine V_x and V_z.

Two of the components of $\mathbf{V}$ can be determined by positioning the (assumed) TCP at three different orientations over a horizontal calibration plane S, see figures 3(b) to 3(d). The calibration plane consist of 2 adjacent plates forming a straight butt seam (sometimes referred to as I-seam). Figure 3(b) shows the z_A-axis of the assumed TCP at right angles with plane S. In this orientation the distance L_0 between the real TCP and the plane S is determined. Next, the robot is rotated over $+\theta_y$ degrees, about the y_A axis of the assumed TCP, see figure 3(c). The distance L^+ between the (new location of the) real TCP and the plane S is determined. Finally, the robot is rotated over $-\theta_y$ degrees, about the y_A axis of the assumed TCP. And the distance L^- of the real TCP to the plane S is determined, see figure 3(c). It follows from figures 3(b) to

3(d) that

$$V_z + L_0 = L^- + V_x \sin\theta_y + V_z \cos\theta_y = L^+ - V_x \sin\theta_y + V_z \cos\theta_y. \quad (2)$$

Rewriting yields,

$$V_x = \frac{L^+ - L^-}{2\sin\theta_y} \text{ and } V_z = \frac{L^- + L^+ - 2L_0}{2 - 2\cos\theta_y} \quad (3)$$

To determine the third component (V_y in this case), the robot must be rotated about the z_A-axis over θ_z degrees, or x_A-axis over θ_x degrees, and expressions similar to equation (3) must be applied. When rotating about the z_A-axis, V_x is obtained, besides the required V_y component. Similar, when rotating about the x_A-axis, V_z is obtained again, besides the required V_y component. Once the three components have been determined a new (calibrated) tool definition is set/defined:

$$TOOL = trans(x, y, z, \varphi, \phi, \rho) : trans(V_x, V_y, V_z, 0, 0, 0) \quad (4)$$

where the operator ':' denotes a compound or combined transformation. That is, the transformation $trans(V_x, V_y, V_z, 0, 0, 0)$ is relative to the coordinate system defined by $trans(x, y, z, \varphi, \phi, \rho)$.

In general, the procedure to determine the components of $\mathbf{V}$, and the definition of the new tool (4), must be repeated serval times, to cope with the non-flatness of the plane S and/or the non-straightness of the seam. The procedure is repeated until all components $V_i, i \in \{x, y, z\}$ are smaller than a predefined value ε. As a result,plane S need not necessarily be horizontal.

Determination of L_0, L^+ and L^- Two methods can be applied to determine the distances L_0, L^+ and L^-.

(*i*) *The move method*: Move the robot, and the sensor, parallel to the z_w-axis of the robot, see figure 2(a), until the real TCP is on the plane S. In this case the z_s value of the sensor indicates zero. The distance traveled by the robot along the z_w axis equals the sought L_0, L^+ or L^-. This method was applied to determine the V_y and V_z components, when rotating the robot about the x_A-axis.

(*ii*) *The measure method*: Once, positioned (figures 3(b) to 3(d)) the distances L_0, L^+ or L^- can be derived directly from the sensor measurements (z_{s0}, z_s^+ and z_s^- or y_{s0}, y_s^+ and y_s^-) using some basic geometry. This method was used to determine the V_x and V_y components, when rotating the robot about the z_A-axis; and to determine the V_x and V_z components, when rotating the robot about the y_A-axis. That is, when rotating about the y_A-axis:

$$L_0 = z_{s0}, L^+ = \frac{z_s^+ \sin(\alpha - \theta_y)}{\sin(\alpha)} \text{ and } L^- = \frac{z_s^- \sin(\alpha + \theta_y)}{\sin(\alpha)} \quad (5)$$

These expressions were substituted into equation (3) to obtain the desired V_x and V_z components.

When, when rotating over θ_z about the z_A-axis, the calibration plane S is defined by a (virtual) plane through the straight seam between the calibration plates. In that case, S is then is perpendicular to these plates. Then, the distances L_0, L^+ or L^- can be determined from the y_s measurements of the sensor,

$$L_0 = y_{s0}, L^+ = y_s^+ \cos(\theta_z) \text{ and } L^- = y_s^- \cos(-\theta_z) \quad (6)$$

These expressions were substituted into the equivalents of equation (3) to obtain the desired components V_x and V_z components.

Error analysis and propagation Summarizing, it can be concluded that 2 methods and 9 orientations of the (assumed) TCP can be used to determine the 3 components V_x, V_y and V_z. To select the method and orientation, which produces the most accurate estimation for each component, the (measurement) errors and their propagation into the expressions for V_x, V_y and V_z were analyzed. Errors in the calibration method are introduced by robot positioning errors, $\Delta_r = \pm 50\mu$m, and measurement errors of the sensor, $\Delta z_s = \Delta y_s = \Delta_s = \pm 40\mu$m (Looman 2000). The robot and sensor errors are assumed to be statistically uncorrelated. Hence, the combined error is estimated by $\varepsilon = \pm\sqrt{\Delta_r^2 + \Delta_s^2} \approx \pm 64\mu$m. The resulting errors in V_x, V_y and V_z are denoted here by $\Delta V_x, \Delta V_y$ and ΔV_z.

It follows from equation (3), that the errors $\Delta V_i, i \in \{x, y, z\}$ due to measurement and positioning errors, increase when the angle $\theta_j, j \neq i$, over which the (assumed) TCP is rotated, approaches zero. However, when the angle θ_j is large, the sensor and/or the focussing optics of the Nd:YAG laser beam may collide with the calibration plane S. Moreover, it was found that the measurement error of the sensor increases significantly when $\theta_j > 35°$. Therefore, the maximum angles, which can be applied are: $\theta_x = 28°, \theta_y = 18°$ and $\theta_z = 35°$. The resulting errors $\Delta V_x, \Delta V_y$ and ΔV_z, can be estimated as (Gaussian fault propagation)

$$\Delta V_i = \varepsilon \sqrt{\left(\frac{\partial V_i}{\partial z_{s0}}\right)^2 + \left(\frac{\partial V_i}{\partial z_s^+}\right)^2 + \left(\frac{\partial V_i}{\partial z_s^-}\right)^2 + \left(\frac{\partial V_i}{\partial y_{s0}}\right)^2 + \left(\frac{\partial V_i}{\partial y_s^+}\right)^2 + \left(\frac{\partial V_i}{\partial y_s^-}\right)^2} \tag{7}$$

Rotation about	Method	ΔV_x	ΔV_y	ΔV_z
y_A-axis	Move	± 96.4	-	± 670.0
y_A-axis	Measure	± 93.1	-	± 662.3
x_A-axis	Move	-	± 146.5	± 1602.4
x_A-axis	Measure	n.a.	n.a.	n.a.
z_A-axis	Move	± 433.7	± 78.9	-
z_A-axis	Measure	± 409.2	± 64.7	-

Table 1: Errors ΔV_i (in μm) for the 2 methods (moving & measuring)

Table 1 lists the numerical values of the errors ΔV_i. It follows from this table that, the component ΔV_x is most accurately determined by rotating about the y_A-axis and using the *measure* method. The component ΔV_y is most accurately determined by rotating about the z_A-axis and using the *measure* method. Finally, the component ΔV_z is most accurately determined by rotating about the y_A-axis and using the *measure* method.

Test of the TCP calibration The method described above was implemented on the controller of the Stäubli RX90 robot, and the TCP of the sensor was calibrated. Next, this TCP was positioned on the seam, i.e. on the plane S. That is, based on the sensor measurements (y_s, z_s and ρ_s), the robot was automatically positioned the sensor until the sensor indicated $y_s = 0$ as well as $z_s = 0$, and $\rho_s = 0$. At this location the robot was used to rotate the sensor about the x_s, y_s, and z_s-axes of the TCP. Figure 4 shows the sensor measurements obtained during rotation. If the TCP was/is calibrated

correctly all sensor signals will stay within the error limits $\pm\varepsilon$. As can be observed from figure 4, this is the case, except for large values of θ_x.

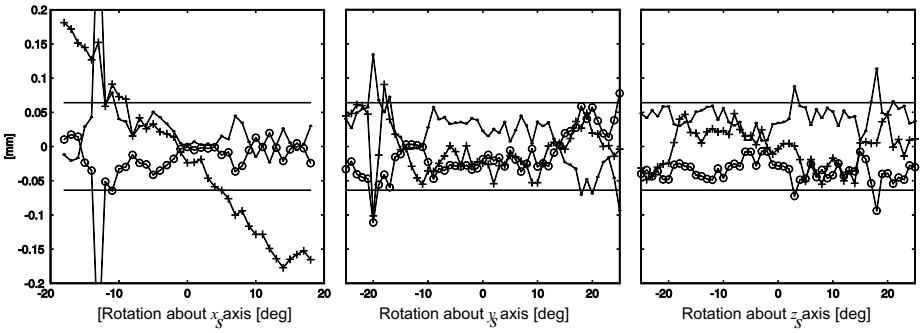

Figure 4: Sensor signals obtained during rotation around the 3 axes of the (calibrated) TCP, after it was positioned on the seam: $\circ = x_s$, $+ = y_s$, $\bullet = z_s$.

Calibration of the TCP of the laser beam The TCP calibration method discussed above, can also be applied to determine the location of the focus of the Nd:YAG laser beam, relative to the face-plate of the robot. However, the seam detection sensor can not be used to determine the distances L_0, L^+ and L^-. In stead the calibration plane S should be replaced by the measurement plane of a *beam analyzer* (Schwede & Kramer 1998). Such a device, measures the intensity profile and diameter of the laser beam in its measurement plane. The focus of the laser beam is characterized by the smallest beam diameter of the intensity profile. Then, using the *move* method, L_0, L^+ and L^- can be determined, and the focus (TCP) can be calibrated.

4 Tracking a seam in 6 coordinates

The need for seam tracking This section discusses a method to track an unknown seam trajectory, prior to welding. That is, on the basis of measurements of the seam detection sensor, the robot guides the sensor automatically and autonomously along the seam. Simultaneously, the 6 (world) coordinates of locations along the the seam are stored in the memory of the robot controller. This method, to automatically program the robot, is usually referred to as *teaching*. The stored trajectory can be replayed, to guide the focus of the Nd:YAG laser beam along the seam for welding. Automatic seam tracking/teaching is significantly more accurate (and less time consuming) than manual teaching of the robot using a teach pendant (joystick).

The tracking algorithm Unfortunately the FALLDORF seam detection sensor generates only 4 coordinates of the seam: 3 translations x_s,y_s, z_s and 1 orientation (angle) ρ_s, whereas 6 coordinates are required to uniquely define a location in world coordinates. The two remaining orientations (angles) can be calculated from two points on the seam.

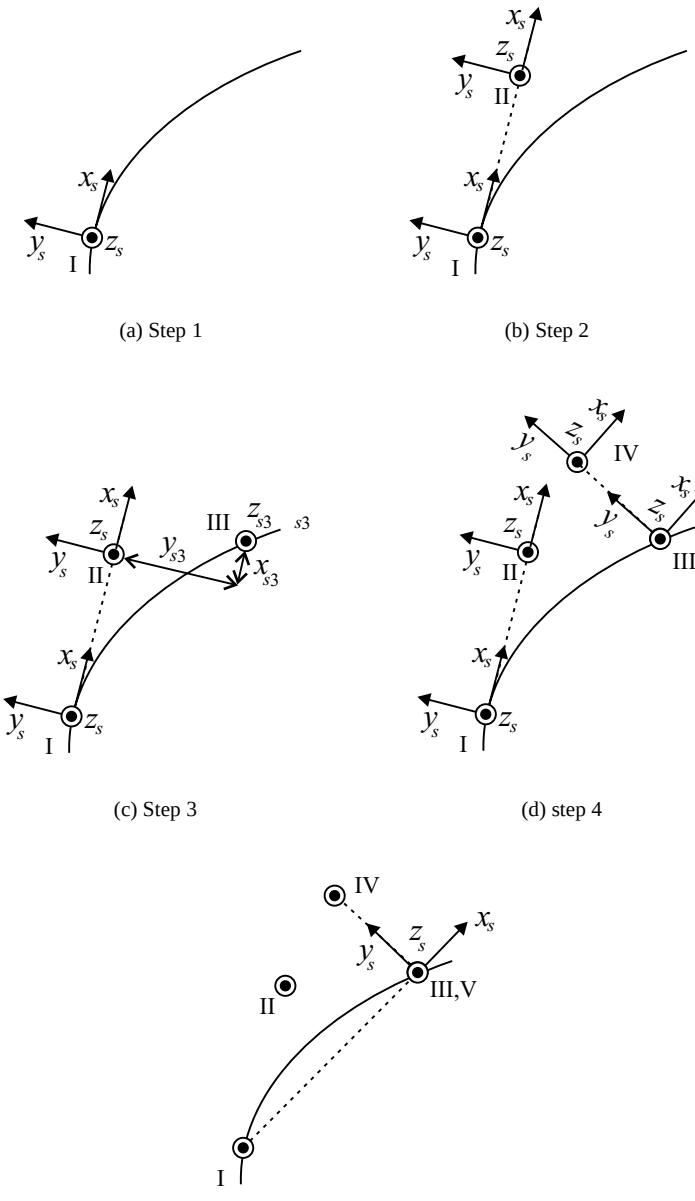

(a) Step 1

(b) Step 2

(c) Step 3

(d) step 4

(e) Step 5 and 6

Figure 5: Steps taken during tracking of the seam

This is illustrated by figure 5 and the following 7 steps:

1. Assume that the TCP of the sensor is on the seam, and that the x_s-axis is tangent to the seam, its y_s-axis perpendicular to the seam and the z_s-axis normal to the surface of the product, see location I in figure 5(a). As the location of the robot face-plate and the sensor tool definition are known (see figure 2(a)), the world coordinates of point I are known. Denote this location (6 coordinates) as *loc1*,
2. Next, the robot translates the sensor along the x_s-axis over a distance Δ, using the command *MOVE loc1:trans(Δ,0,0,0,0,0)*. Then the coordinate system of the sensor is aligned as in location II, see figure 5(b). Denote this location as *loc2*,
3. At *loc2*, the seam (location III) can be measured using the seam detection sensor. Suppose, that at *loc2*, the sensor indicates x_{s3}, y_{s3}, z_{s3} and ρ_{s3}, see figure 5(c). Then calculate $loc3$ as $loc3 = loc2 : trans(x_{s3}, y_{s3}, z_{s3}) : RX(\rho_{s3})$. Where RX($\cdot$) denotes a rotation about the x-axis. The origin of $loc3$ is at location III, and its ρ_s signal will be zero. However, the x-axis of $loc3$ is not tangent to the the seam.
4. A fourth location $loc4$ is calculated: $loc4 = loc3 : trans(0, \Delta, 0, 0, 0, 0)$. This location has the same orientations as $loc3$, but is shifted over Δ along the y-axis of $loc3$, see figure 5(d).
5. Next, a so called $FRAME$ function is used to calculate $loc5$, that is $loc5 = FRAME(loc1, loc3, loc4, loc3)$. The function $FRAME$ returns 6 (world) coordinates of a location (here $loc5$) with:
   - its origin in $loc3$
   - its positive x-axis parallel to the line passing through points defined by $loc1$ and $loc3$, in the direction from $loc1$ to $loc3$,
   - its XY-plane parallel to the plane that contains the points defined by $loc1$, $loc3$ and $loc4$,
   - its positive y-direction is from the x-axis as defined above, towards $loc4$.
6. The robot is instructed to move to $loc5$. The sensor is now positioned and oriented as shown in figure 5(e). This location is stored in memory of the robot controller for later replay.
7. Goto step 1, and consider the current location ($loc5$) as $loc1$. That is $loc1$ is redefined: $loc1$=$loc5$.

As can be observed from figure 5(e), the x_s-axis of $loc5$ will only be tangent to the seam if Δ is small compared curvature of the seam.

Testing the seam tracking algorithm A plate with a sinusoidal seam trajectory was placed in the robot envelope. The plate was oriented arbitrarily with respect to the world axes of the robot. The teach pendant was used to position the robot, such that the seam detection sensor was at the start of the seam. Next, the seam tracking algorithm was started. Figure 6(a) shows the recorded locations along the seam. The recorded locations were replayed by the robot. Figure 6(b) shows the sensor measurements obtained during replay (as the x_s measurement is not relevant, it is not displayed here). If the seam was tracked correctly the sensor signals will stay within the error limits $\pm\varepsilon$. As can be observed, this is the case. The measured $\rho_s \in [-1, 1]$, is well within the measurement accuracy of this angle.

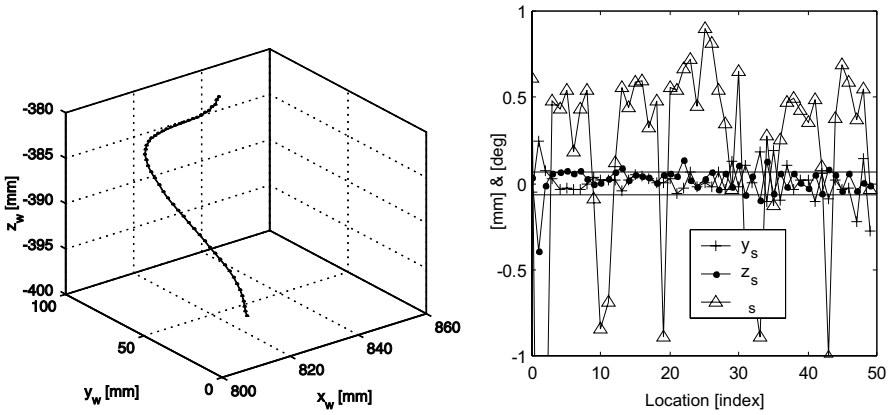

(a) World coordinates of the tracked/recorded seam.

(b) Sensor readings obtained during replay of the recorded seam.

Figure 6: The tracked seam and the sensor readings during replay of the recorded locations.

5 Conclusions

A method for TCP calibration of a seam detection sensor was presented and tested. The accuracy of the method is estimated at approximately $\pm 70\mu$m. A method to track/teach a 3D seam within the robot envelope was presented and tested. The accuracy of stored/taught locations along the seam is also estimated at approximately $\pm 70\mu$m. These results are well within the demanded accuracy of 100μm for laser welding.

Acknowledgement The practical support of Christian J. Boer during the experiments is greatly acknowledged.

References

Looman, W. (2000). *Seam teaching for laser welding with the FAMM using the falldorf seam detection system*, Master's thesis, University of Twente, Deptart of Mechnical Engineering, Enschede, the Netherlands. Internal report WA702.

OldeBenneker, J. (2000a). Evaluatie van de panasonic VR008AE robot voor het laserlassen, *Technical Report Intern rapport WA-673*, Universiteit Twente, Enschede.

OldeBenneker, J. (2000b). Toelaatbare toleranties bij het laserlassen van aluminiumlegeringen, *Technical Report WA-683*, Universiteit Twente, Enschede. PMP rapport GA00-18.

Schwede, H. & Kramer, R. (1998). High performance laser beam diagnostics in industrial environment, *Proceedings of the ICALEO98*.

Thorne, H. (1999). Tool center point calibration for spot welding guns. US patent US5910719.